Colloid Polym Sci 275:352–363 (1997)
© Steinkopff Verlag 1997

ORIGINAL CONTRIBUTION

M.L. Janex
V. Chaplain
J.L. Counord
R. Audebert

Influence of adsorbed polymers on the removal of mineral particles from a planar surface

Received: 16 February 1996
Accepted: 10 September 1996

M.L. Janex · R. Audebert
Laboratoire de Physicochimie
Macromoléculaire
de l'université Pierre et Marie Curie
CNRS URS 278
10, rue Vauquelin ESPCI
75231 Paris, France

Dr. V. Chaplain (✉)
Unité de Phytopharmacie
et Médiateurs
Chimiques INRA
Route de Sanit-Cyr
78026 Versailles, France

J.L. Counord
Laboratoire de Biorhéologie
et d'Hydrodynamique Physicochimique
Université Paris VII
CNRS URA 343
2, place Jussieu
75451 Paris, France

Abstract Experimental results on the role of adsorbed polymers on the particle adhesion are presented. Both Brownian (silica particles) and non-Brownian (glass beads) particles were used. The particles were deposited onto the internal surface of a glass parallelepiped cell, and then submitted to increasing laminar flow rates. The pH and the ionic strength of the electrolytes were fixed. The adhesive force was related to the hydrodynamic force required to dislodge 50% of the initially attached beads. We found that high molecular weight PEO had little effect on the adhesion of small silica beads due to the low affinity of the polymer for silica or glass surfaces. On the contrary, PEO greatly enhanced the adhesion of bigger glass beads forced to deposit on the capillary surface because of gravity. The increase was all the more pronounced as the molecular weight of the polymer was high. The effect of high molecular weight cationic copolymers on the adhesion of silica particles was drastic. The maximal force (1500 pN) applied by the device could not enable any particle detachment even using polymers of low cationicity rate (5%), showing the efficiency of electrostatic attractions. When copolymers were adsorbed on both surfaces (particles and plane), the adhesive force exhibited a maximum at intermediate coverage of particles. This optimum was related to the optimum flocculation concentration classically observed in flocculation of suspensions by polymers.

Key words Particle adhesion – polymer adsorption – flocculation – zeta potential polyelectrolyte

Introduction

Ultrafiltration membranes have been recently developed as a new process in the drinking water industry. The raw water is driven inside hollow fibers: materials bigger than the pore size, around 10 nm, are excluded, enabling clarification and disinfection of the raw water. The major limitation of this high performing method is linked to the progressive fouling of the membrane, despite regular backwashings and the possible tangential circulation of the water inside the fibers. Fouling is a complex mechanism, involving different phenomena such as adsorption, concentration polarization, and material transfer [1]. It was observed that raw waters containing organic and mineral matter altogether lead to high fouling. This synergetic effect was attributed to the formation of an adsorbed polymer layer on the mineral surface which induces both a decrease of the filtration cake porosity and an increase of interparticle aggregation forces [2].

In this study we investigated the influence of polymer adsorption on the adhesive force between mineral surfaces. Force measurements are of interest because they can provide insight not only into fouling effects but also into fundamental problems of particle adhesion involved in flocculation by polymers. Various industrial processes are concerned such as mineral coal processing, paper-making, water and waste water treatment. These interactions also play a major role in biological systems [3, 4] and in cohesion of soils [5].

Surface force apparates

Developments in the measurement of interparticle or intersurface forces have been recently reviewed [6]. As the interaction between real particles (a few microns in size, or less) cannot be directly measured, corresponding sphere/plate [7–9] or crossed cylinders [10] models are usually applied. The sophisticated surface force apparatus developed by Israelachvili [11] or its derivatives based on the same principle [10] and atomic force microscopes provide experimental "force-distance" profiles. These profiles agree with the classical D.L.V.O. theory [12] when distance between surfaces is greater than a few nanometers. But short range-repulsions have been evidenced when molecular effects become dominant [13]. Information about the charging mechanism of surfaces due to a modification of the pH can also be derived from the force measurements. Experimental results were qualitatively expressed in terms of the roughness of surfaces, which increases the effective separation at aperity contact [14]. As far as polymers are concerned, most of the experiments were performed with fully covered surfaces because of experimental constraints [10, 15–19]. Different parameters were studied, such as the molecular weight of the adsorbed polymer [20, 21], its nature, its charge [22, 23], its concentration in the solution [20, 21], the solvent quality (usually good solvents were used [22]), or the ionic strength of the medium [24–29]. Such experimental studies aimed at the determination of the steric interaction range, providing insight into layer thicknesses and chains conformations [30]. In very few cases the surfaces were not identically covered [31], or not completely covered [32, 33]. Strong attractive interactions were then attributed to bridging.

Hydrodynamic detachment methods

Most of the methods aiming at adhesive force measurement are based on the hydrodynamic detachment of spherical particles from plane solid surfaces. The adhesive force is then defined as the tangential hydrodynamic force required to dislodge a given amount (usually 10 or 50%) of the initially deposited particles. Various geometries were used such as coaxial cylinders [34], cylindrical [35] or square tubes [36]. The plane surface could also be subjected to a stagnation point flow [37]. Some authors [33] also used a centrifugal technique, where the direction between the force exerted on the adhering particles and the plane surface could be chosen from tangential to perpendicular. Previous detachment studies pointed out the influence of some parameters on particle adhesion. For instance, Visser [34, 38] showed that the detachment force required to dislodge carbon black and polystyrene particles from cellulose depended on variables such as pH and ionic strength. Results also differ according to the nature of the substrates and the size of the particles [33, 39–41]. Several detachment experiments involving polymers are described in the literature. In most of them polymer was adsorbed on a single surface and this enhanced particle adhesion. Mühle et al. [33] observed a continuous increase of the adhesive force with the polymer concentration used in the adsorption step while Pelton et al. [32] observed a maximum followed by a decrease. The increase of the molecular weight is usually found to enhance particle adhesion [32, 33]. Hubbe et al. [42] reported that the force required to detach TiO_2 particles from glass surfaces which were fully covered by cationic copolymers decreased when the cationic charge of the copolymer increased. Very few results are available where both surfaces (particles and plane) are covered with polymers. Van de Ven et al. noted that no deposition of Brownian particles occurred when both surfaces were coated with a cationic polymer [43]. Actually, drawing conclusions from those various results is not easy because of some fundamental parameters which differ from one experiment to the other. Among them are the size and the weight of the particles, their elasticity (rigid or deformable), all of which affect the release mechanism. Furthermore, the flow imposed to detach particles can be laminar or turbulent. Eventually, apart from results obtained with latex particles, all the reported detachment curves reveal a broad distribution of the adhesive forces within a population of beads.

In this study, we chose a method based on the hydrodynamic detachment of spherical particles to get a better insight into the role of adsorbed polymers in the adhesion of rigid particles. Particles were deposited inside plane glass capillary tubes of rectangular section. Experiments were performed both with Brownian silica particles and with non-Brownian glass beads. The flow was always kept laminar. The ionic strength and the pH of the flowing solution were controlled. We used high molecular mass polyethylene oxides and cationic copolymers of various charge. In our method, both surfaces were prepared separately, thus we could use surfaces covered with unequal amounts of polymer.

We first report about the measurements we performed with bare surfaces, which provided a reference value of the

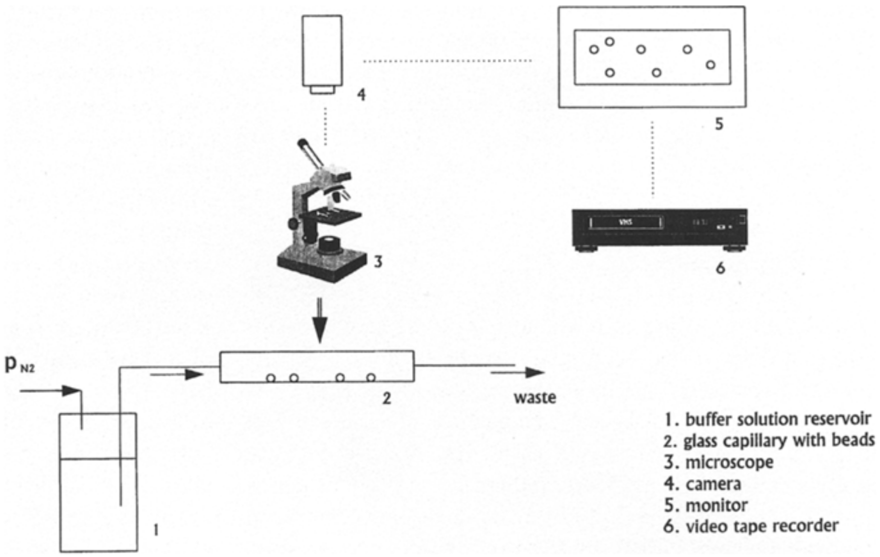

Fig. 1 Schematic diagram of the device

adhesion force. The influence of polymers was then analyzed when a single surface was covered with polymer, distinguishing different cases according to the nature of the polymer and the size of the beads. We eventually developed the results obtained when polymers were adsorbed on both surfaces, and the detachment experiments were related to the flocculation phenomena observed in suspension.

Experimental

Experimental setup

A schematic diagram of the experimental setup is depicted in Fig. 1. Particles to investigate were injected into a glass capillary. The capillary, being maintained in a rigid cell, was placed on the stage of a microscope (Olympus) fitted with a ×40 long-working distance objective, so that the particles could be observed inside the capillary. The microscope was linked to a Hamamatsu video camera, a monitor and a Sony video recorder. So, the detachment of beads was continuously recorded during the elution of the electrolyte. The cell could receive two capillaries simultaneously, which made comparative measurements easier. The borosilicate glass capillaries, supplied by Vitro Dynamics, were 300 mm long and had rectangular sections. Three different cross-section sizes were available: width and thickness (w, 2b) were respectively (6 mm, 300 μm), (4 mm, 200 μm) and (2 mm, 100 μm). Capillaries were connected through inert Teflon tubes to a 5-l reservoir (Amicon) containing the electrolyte solution at room temperature. A constant N2 pressure, between 1 to 5 bars, could be applied in the reservoir producing controlled flow rates through the capillary. Additional metallic tubes, placed between the reservoir and the capillaries, extended the range of the available flow rates. Corresponding data are indicated in Table 1. To assure a laminar flow inside the

Table 1 Available dimensions of beads and capillaries with corresponding forces applicable with the device

Width of the capillaries w, in mm	Thickness of the capillaries 2b, in μm	Diameter of beads, in μm	Range of the flow rate Q, in ml/mn	Range of the tangential force F_h, in pN	Lift force/F_h at maximum flow rate
6	300	20	0.05 to 66	20 to 26500	0.24
		1.5		0.1 to 150	$1.3\ 10^{-3}$
4	200	20	0.05 to 45	not used	
		1.5		0.6 to 600	$1.9\ 10^{-3}$
2	100	20	0.05 to 23	not used	
		1.5		3 to 1500	$1.3\ 10^{-2}$

Table 2

Cleaning procedure of bare surfaces of capillary tubes	
Oxonia 2% + US	40 min
Milli Q water	15 min
KNO_3 2M	40 min
electrolyte of the specific experiment	2 h

capillary, the maximal value of the Reynolds number Re was 100, where Re is defined as $Re = vb/\nu$ (v: average velocity of the fluid in the capillary; ν: kinematic viscosity of the fluid). Each flow rate was precisely measured by weighing and timing within an error of 1%.

Calculations

The particles were observed at about 150 mm from the inlet of the capillaries, which was more than the inlet distance l_i required to get an established laminar profile ($l_i = 0.09$ Re.b (44), $l_i = 9b$ at maximum flow rates). Then we could consider the hydrodynamic flow as laminar in the area of observation. This laminar flow could be described by a flat velocity profile in a horizontal plane and a parabolic velocity profile in the vertical plane. The tangential hydrodynamic force applied on a sphere attached to a wall, F_h, was calculated by Goldman et al. [45] as a function of the Stokes drag force F_{st} in an infinite sea of liquid:

$$F_h = 1.7\,F_{st} = 10.2\,\pi\mu r v_r = 10.2\,\pi\mu r 1.5\bar{v}\left(1 - \left(\frac{b-r}{b}\right)^2\right) \tag{1}$$

where μ is the viscosity of the electrolyte, v_r the fluid velocity at one particle radius r from the wall and $\bar{v}$ the average fluid velocity in the section of a capillary. The range of F_h is given in Table 1 for particles of diameter 1.5 and 20 μm. The relative error on F_h arose from those on the flow rate, the dimensions of the capillaries and the size of the beads. It was evaluated to 8%. The lifting force F_n acting normal to the plane surface was usually negligible. Ratio values of F_h/F_n are given in Table 1.

In a typical experiment, capillaries were cleaned following the procedure described in Table 2. Then a dilute suspension of beads was injected inside the capillary to give a sparse coating of the glass surface (the distance between 2 neighbouring particles had to be bigger than 3 diameters [44]). Between 130 to 200 (N_0) particles were initially counted after a settling time of about 40 min. Particles were submitted to 10 min sequences of controlled flow rate. At the end of each sequence the number (N) of remaining beads was counted. This duration was enough to get an unchanged number of detached particles. Moreover, the number of particles detached at a given flow rate did not depend on the flow rates previously applied. Results were plotted as the fraction of released particles against the applied hydrodynamic force F_h. The adhesive force F_a was defined as the force required to dislodge half of the initial deposited particles (N_0). The relative error on particle counting was 2%, then that on the adhesive force was 10%.

The distribution factor, σF, characterized the distribution of the adhesion forces around F_a:

$$\sigma F = \frac{F_{80} - F_{20}}{F_{50}} \tag{2}$$

where F_{80} and F_{20} were the forces required to dislodge 80% and 20% of the initial beads, respectively.

Beads

Most of the detachment experiments were performed with non porous synthesized silica beads of average diameter 1.5 μm (±2%) and density 2.2. Particles were kindly provided by B. Sébille [46]. For some comparative measurements, we used bigger glass beads: average diameter 20 μm (±4 μm), same density. Before use, the beads were cleaned and rinsed in successive steps by several sequences of centrifugation or decantation (depending on their size) and redispersion in the adequate electrolyte. Silica particles, referred to as Pst 1, purchased from Nissan Chemicals Industries, were used in polymer adsorption studies for their higher specific surface area (22 mg/m^2). Their hydrodynamic radius measured by QELS was 60 nm. The cleaning of such suspensions by ultrafiltration after treatment by H_2O_2 has been previously described [47].

Electrolyte solution

All solutions and suspensions were prepared in maleic acid buffer of pH6. The various ionic strength values I were imposed by the buffer concentration. That buffer was made from deionized water (milli-Q system from Millipore).

Polymers

As neutral polymers, we used three commercial polyoxyethylene samples (Aldrich) of nominal molecular weight 2 10^6, 600 000 and 35 000 designated as PEO2M, PEO600 and PEO35. The polyelectrolytes were two cationic copolymers of acrylamide synthesized in our laboratory and whose characteristics have been given previously [47]. Their general formula is given below:

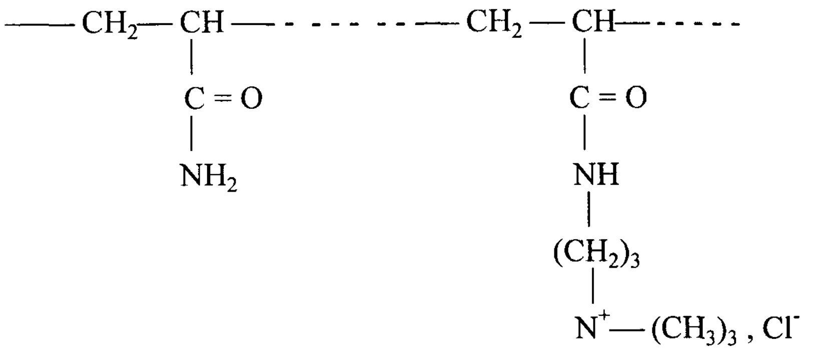

$$-CH_2-\underset{\substack{|\\ C=O\\ |\\ NH_2}}{CH}-\cdots\cdots-CH_2-\underset{\substack{|\\ C=O\\ |\\ NH\\ |\\ (CH_2)_3\\ |\\ N^+-(CH_3)_3,\ Cl^-}}{CH}-\cdots$$

The crucial parameter is their cationicity rate, τ, which is the molar ratio of cationic monomers randomly distributed along the chain. Two samples were used referred to as cat5 ($\tau = 5\%$) and cat100 ($\tau = 100\%$) respectively. The average molecular mass values $M_w = 1.1\ 10^6$ for cat5 and 300 000 for cat100 were derived following a procedure previously described [48].

Preparation of the polymer-coated surfaces

Beads and capillary surfaces were prepared separately. Dilute samples ($\cong 0.14$ g/l) of small beads were prepared corresponding to various polymer doses. Samples were gently stirred and left at rest for 20 min before injection into the capillary. Saturation on beads with PEO 2M required a larger time (a few hours), to allow the progressive exchange of chains of different molecular weight before reaching the equilibrium. Then the beads were rinsed from the excess of polymer by successive stages of centrifugation and redispersion.

When covered with polymer, the capillary surface was always saturated. A polymer solution (200 ppm) was slowly pumped in the capillary during more than 10 h. The flow rate was such that the wall shear rate was smaller than 25 s^{-1} to limit any disturbance of the polymer layer, which might occur with shear rates bigger than 2500 s^{-1} [49]. After adsorption, the excess of polymer was removed by slow elution of the electrolyte solution, during 2 h. This enabled the elution of more than 20 times the volume of the capillary, which guaranteed a good rinsing. After an experiment with polymer adsorbed on either surface, the capillary could not be used again as a bare surface for a following experiment, so the capillary had to be renewed.

Electrophoresis

The electrophoretic mobility of particles was measured at room temperature using the zetaphoremeter II (Sephy). The electrophoretic mobility was then converted to the zeta-potential value using the Smoluchovski law. Additional measurements were made using the laser Zee Meter model 3000 (Pen Kem Inc.). This device gave the distribution of the electrophoretic mobilities of a particle sample. Spectra were characterized by the mobility value of the highest peak and by the width at half-height. Good agreement was found with the two devices.

Quasi elastic light scattering

The Stokes radii of covered and bare silica Pst1 particles were determined by using a homemade QELS device including a Malvern correlator. The hydrodynamic polymer layer thickness was derived from the difference between the two radii. Dilute suspensions (0.01 g/l) at pH 6 and ionic strength $I = 10^{-3}$ M were used. A large excess of polymer was brought without shaking to avoid any particle aggregation during the polymer adsorption stage. QELS measurements were performed at various diffusion angles and confirmed the absence of aggregates.

Results and discussion

Adsorption of polymers on particles

Adsorption of neutral PEO on silica Pst1 particles was characterized by a round shape isotherm curve due to the preferential adsorption of larger chains [47]. The maximal amount Γ_{max} was 1.1 mg/m^2. On the contrary, adsorption of the polyelectrolytes lead to very high affinity isotherms. The plateau values were 0.5 and 1.2 mg/m^2 with cat100 and cat5 respectively. In each case, the coverage rate, Γ, of the particles was controlled by the polymer dose, Ci/S, which is the mass of polymer initially introduced per total available surface of beads [47].

The hydrodynamic layer thickness δ_h of saturated Pst1 silica particles was measured by QELS. Both PEO 2M and cat 100 polymers adopted a flat conformation leading to a low value of the polymer thickness $\delta_h = 10$ nm. On the contrary the cat5 copolymers could develop large loops because the neutral monomers did not adsorb on the silica surface. The polymer thickness reached 75 nm.

Flocculation induced by polymers

Previous results have seen that neutral PEO 2M was able to flocculate colloidal Pst1 silica suspensions providing the particle concentration was high enough. Particle aggregation occurred through a non-equilibrium bridging, especially at low polymer dose. In contrast to this, flocculation by polyelectrolytes occurred with a very high efficiency, even in very dilute suspensions because of attractive interactions between partially covered particles [47]. The flocculation area ranged from 0.75 to 0.95 mg/m^2 with cat5 and 0.1 to 0.3 mg/m^2 with cat100 in dilute suspensions under quiescient conditions. Particles were stabilized again above those ranges of polymer dose because of steric and electrostatic repulsions between adsorbed chains.

Change of zeta-potential of Pst1 particles induced by polymer adsorption

The adsorption of a neutral polymer on a negatively charged surface decreased the ζ-potential value. This decrease was all the more pronounced as the molecular weight of the polymer was high. The zeta-potential of Pst1 particles turned from -50 mV without polymer to $\xi_{max} = -35$ mV when particles were completely covered with PEO 35 and approached zero when covered by PEO 2M. Note that an excess of PEO 2M polymer was required to get the maximum value ξ_{max} due to the polydispersity effect [47].

When silica particles were progressively covered by cationic copolymers, their global charge reached a positive value. This could be well described in Fig. 2 by the evolution of ζ-potential of silica particles Pst1 outside the flocculation range. The maximum value of ζ-potential was $+10$ mV with cat5 copolymer and $+23$ mV with cat100 polymer. These maximum values were reached as soon as the polymer dose was equal to Γ_{max}. Exchange of small chains by larger ones did not occur with these polymers because of the high affinity of the cationic monomers for the surface. Taking into account the amount of adsorbed polymer at saturation and the cationicity rate for each polymer, the number of positive charges brought by the cat 100 polymer was 10.8 times (3.4 times with the cat5 copolymer) the number of negative charges carried by the bare particles. Despite the large excess of cationic groups, the maximum value of the ζ-potential reached a low positive value compared to the high negative value of the bare particles. As for neutral polymers, the thickness of the polymer layer affected the value of the zeta-potential so that external charges predominantly contributed to the zeta-potential value. The volume distribution of charges inside the polymer layer could also have a significant effect through a possible condensation of charges when the cat100 polymer was involved [50]. As a consequence, the difference between the two polymers cannot just be explained by their difference of charge rate.

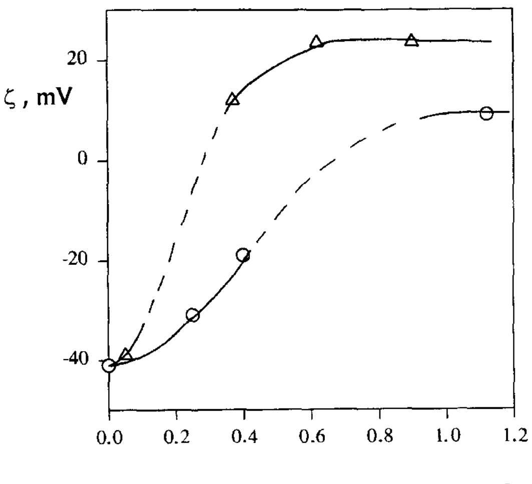

Fig. 2 Variation of the ζ-potential of silica particles PST1 with the dose C_i/S of the poly-electrolytes cat5 (○) and cat100 (△) (C_i is the initial polymer concentration, S is the total surface of particles per unit volume). The dotted lines indicate the flocculation area where ζ-potential cannot be measured (from 0.6 to 0.8 mg/m^2 with cat5 and 0.1 to 0.3 mg/m^2 with cat100). $I = 10^{-3}$ M and pH = 6, in maleic buffer

The width of electrophoretic mobility of Pst1 silica suspensions is shown in Fig. 3 as a function of the amount of adsorbed cat5 cationic copolymer. Copolymer saturation always lead to very thin spectra. A similar behaviour was observed with the cat 100 polymer. Quantitatively, the electrophoretic mobility of bare particles was characterized by a standard deviation of 0.1, whereas it fell to 0.02 for saturated particles. Adsorption of polymers induced changes in charge densities. If negative charges might be inhomogeneously scattered all over the surface, charges brought by polyelectrolytes appeared able to mask inhomogeneities of the bare surface.

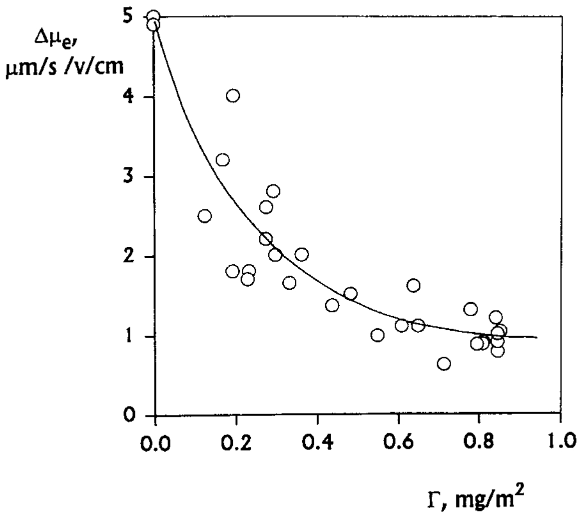

Fig. 3 Variation of the width of the electrophoretic mobility spectra of silica particles PST1 as a function of the amount of copolymer cat5 adsorbed ($I = 10^{-3}$ M and pH = 6, in maleic buffer). The width of spectra was measured using the laser Zee Meter model 3000 (Pen Kem Inc.). Saturated particles always led to very thin spectra

Adhesion of bare particles on bare surfaces

A few results were obtained with the bigger beads, which could deposit on the capillary surface under the action of gravity whatever the pH and ionic strength conditions. At pH 6 and $I = 10^{-3}$ M more than half of the beads were dislodged when applying the minimum available hydrodynamic force, which was 20 pN for such a bead size. We kept this value as our reference adhesive force obtained without polymer.

Measurements performed with small silica beads at pH 6 showed that deposition was sensitive to ionic strength. At low ionic strength ($I = 10^{-3}$ M) electrostatic repulsions between both negatively charged surfaces were such that they prevented any adhesion. Particle adhesion was made possible when the ionic strength was greater than 10^{-2} M, for which negative surface charges were screened. A great number (greater than 20) of experiments was repeated at pH 6 and $I = 6.4\,10^{-2}$ M. Most of them led to an adhesive force value around 50 pN. Some of them are reported by straight lines in Fig. 4. A few curves exhibit higher values (dotted lines on Fig. 4) revealing that the surface charge could not be easily controlled, despite the drastic cleaning and rinsing procedure we used. We kept 50 pN as reference value for the adhesive force between small silica beads and a bare glass capillary at pH 6 and $I = 6.4\,10^{-2}$ M.

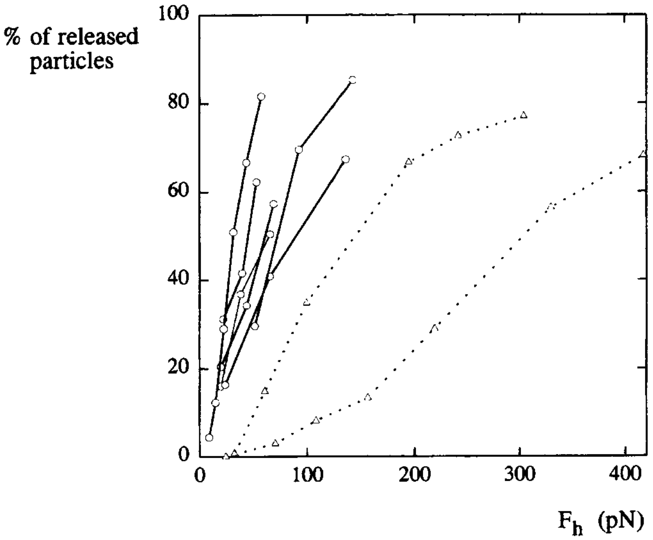

Fig. 4 Experimental detachment curves of silica particles deposited on the bare glass surface of the capillary at pH 6 and ionic strength $I = 6.4\,10^{-2}$ M imposed by the maleic buffer. Curves show the % of released particles as a function of the increasing hydrodynamic force F_h applied on the particle by the laminar flow. Most of the experiments led to an adhesive force F_a of 50 pN. The distribution factor σF defined in Eq. (2) is close to 1 for each experiment. Dotted lines indicates non reproducible data which cannot be discarded despite the drastic experimental procedure

Adhesion of bare particles and surface roughness

The definition of the adhesive force we used is quite arbitrary since the relationship between the applied tangential force and the adhesive force, which acts normal to the wall is not really understood. It was previously concluded that the detachment of rigid spherical particles from a bare rigid surface was initiated by rolling rather than sliding [51–53]. Asperities on either of the surfaces in contact may act as resistant points against rolling [52]. In our experiments, we investigated the roughness of the surfaces by electronic microscopy. The characteristic length was estimated around 10 nm for silica beads, glass beads and capillaries. This typical length is small when compared to the particle size, which accounts for the low values of the adhesive force we found.

Roughness also accounted for distributions in the adhesiveness of individual particles in an adhering population [51]. The distribution of the adhesive force was characterized by the factor σF, defined in Eq. (2), and was close to 1 in our experiments, compared to between 1 and 6 as calculated from others reports [32, 33, 37, 43]. The low value of σF in our case could be attributed to a rather small size distribution of the beads, which were very monodisperse, and to the low roughness of the surfaces.

A parallel could also be drawn between particle detachment and ζ-potential. So the force distribution could be compared to the width of the electrophoretic mobility spectra, and thus reveal an inhomogeneous repartition of charges throughout the surfaces.

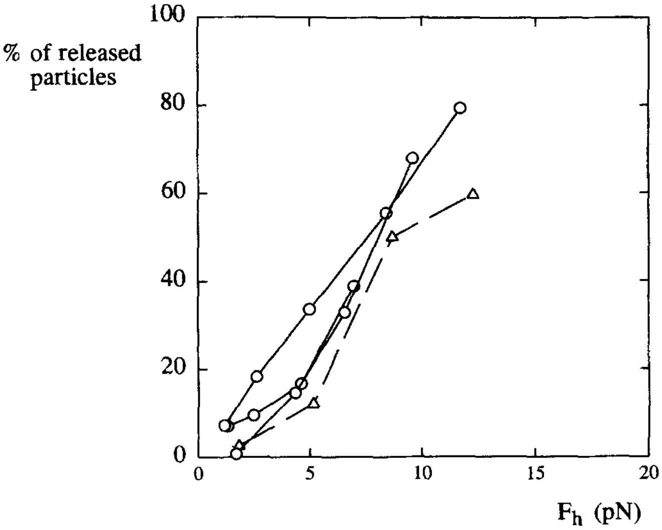

Fig. 5 Experimental detachment curves of silica particles covered with PEO 2M prepared at 0.14 g/l and then deposited on the bare glass surface of the capillary. The adhesive force derived F_a is 8 ± 1 pN. The factor distribution σF is around 0.8. The value of the adhesive force is not changed when the deposit time of particles before detachment experiment is increased from 45 to 60 min as indicated by dotted lines. (pH = 6, $I = 10^{-3}$ M, in maleic buffer)

Influence of the molecular weight of PEO on the adhesion of particles of different sizes

PEO was adsorbed on the beads surface whereas the capillary surface was initially bare. If care was taken to avoid aggregation during the polymer adsorption stage, then the reproducibility of measurements was greatly enhanced as compared to the experiments performed with both bare surfaces. Experimental results show a very distinct behaviour according to the size of the beads. For the smaller beads, the influence of PEO was studied in two media of different ionic strengths:- low ($I = 10^{-3}$ M) where electrostatic repulsions prevented the deposition of the bare beads on the bare surface of the capillary–moderate ($I = 6.4\,10^{-2}$ M) where adhesion was observed even without any polymer ($F_a \approx 50$ pN). For the larger glass particles, experiments were performed only at pH 6 and ionic strength 10^{-3} M for which the reference value of the adhesive force F_a was 20 pN.

In the first case of low ionic strength, the adsorption of a neutral polymer did not change the electrostatic repulsions between charged surfaces. Thus adhesion was expected when the adsorbed polymer layer was thick enough as compared to the minimum separation distance between surfaces imposed by the electrostatic repulsions. Actually, adhesion of small silica particles was made possible by completely saturating the surface of the beads with a high molecular weight polymer, the PEO 2M. Figure 5 shows the increasing fractions of released particles as a function of the force imposed by the flow. An adhesive force $F_a = 8 \pm 1$ pN can be deduced. A similar value was found if the detachment procedure began 60 h after the deposition of the beads onto the capillary surface (dotted line in Fig. 5) showing no strengthening of the adhesive force with time. This low value reveals the small affinity of PEO segments for the glass surface. At moderate or low coverage with PEO 2M, or at full coverage with a smaller PEO ($M_w = 600\,000$), particles did not attach to the glass surface.

In the second case of moderate ionic strength, the adhesive force was hardly modified by the presence of PEO adsorbed on the beads. The molecular weight slightly influenced the detachment of the particles. The adhesive force F_a measured was 30 pN with particles saturated by PEO 35 and 55 pN with PEO 2M. Two competitive effects have to be considered: i) macromolecular chains act as bridges between the two surfaces, which enhances particle adhesion, and ii) the pressure exerted on the polymer layer due to the weight of particles is very low (gravity of the particles being around 0.4 pN), involving no disturbance into the polymer layer when both surfaces approach. So the adsorbed polymer layer, which can be several nm thick with PEO 2M, spaces out the surfaces. Both opposite effects–bridging and spacing–increase with the molecular weight of the polymer. Those competitive effects associated with the low affinity of PEO segments for the glass surface could explain the small variations of the adhesive force when compared to the reference value measured between bare surfaces.

The effect of adsorbed PEO on the adhesion of the bigger glass beads onto the plane surface was completely different, as can be seen in Fig. 6. The adhesive force deduced from experiments was 150 pN with PEO 35 (Fig. 6a) and 3000 pN with the PEO 2M sample (Fig. 6b) and had to be compared with an adhesive force lower than 20 pN without polymer. The increase was all the more pronounced as the molecular weight of the polymer was high. Such an effect is in agreement with analogous results obtained with neutral polymers on the same big glass beads [44]. For big particles, the flattening of the polymer layer under the pressure exerted by the particles (the gravity is around 50 pN) increases the density of links between the two surfaces, while the distance between them is not significantly changed compared to the bare situation. As

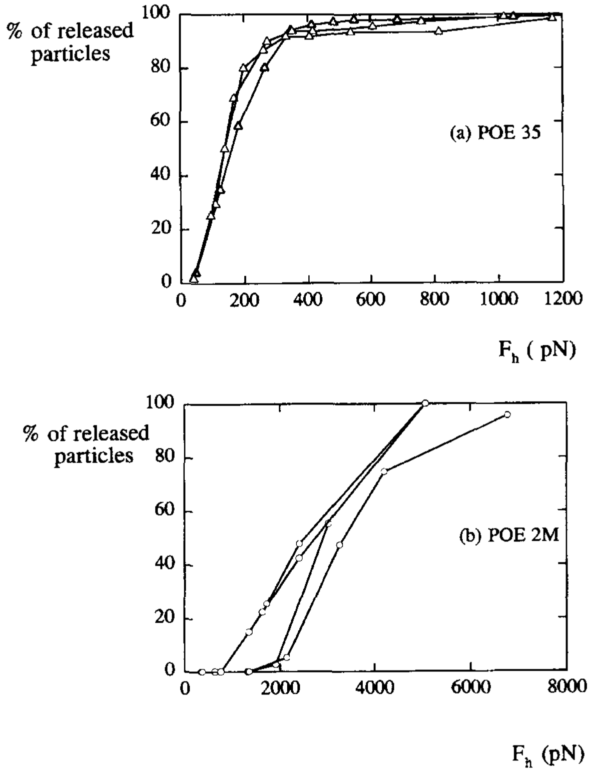

Fig. 6 Experimental detachment curves of glass beads fully covered by PEO and initially deposited on the bare surface of the capillary. Curves show the influence of the molecular weight of the polymer on the adhesive force. F_a is 150 pN with a molecular weight M_w of 35 000 (Fig. 3a) and $F_a = 3000$ pN with $M_w = 2\,10^6$ (Fig. 3b), (pH = 6, $I = 10^{-3}$ M, in maleic buffer)

a consequence the adhesion is all the more pronounced as the molecular weight of the polymer is high.

Influence of polyelectrolytes on particle adhesion

All experiments were performed at the same pH = 6 and an ionic strength 10^{-3} M. Cationic copolymers were expected to attach particles to the glass surface, even under unfavorable low ionic strength conditions, thanks to electrostatic attractions between oppositely charged surfaces. Actually, with cat5 fully covered particles, the effect was drastic: the particle attachment was so much enhanced that the maximal force (1500 pN) applied by the device could not enable any particle detachment. But below 0.4 mg/m^2 particles still appeared as negatively charged with a negative value of the ζ-potential ($\xi = -20$ mV, see Fig. 2). They did not deposit onto the glass surface.

In the symmetric situation, bare particles spontaneously attached to the fully covered capillary surface. Figure 7 shows the detachment of bare particles when the capillary was covered with polymer cat5 or cat100. The measurements pointed out the dissymmetry between opposite situations (covered capillary/bare beads and bare capillary/covered beads) with the cat5 copolymer. The adhesive force F_a was higher than 1500 pN with saturated particles and equal to 650 pN when the capillary was fully covered. A difference in the affinity of copolymers for silica or glass surfaces could explain such an effect. The increase of the cationicity rate from 5% to 100% enhanced the particle adhesion. The adhesive force was 1300 pN with the cat100 polymer. But as for zeta-potential measurements, the difference between the two polymers is low compared to the difference of their cationicity rate. This correlation between both types of measurements suggests that they both predominantly depend on the number of external cationic groups.

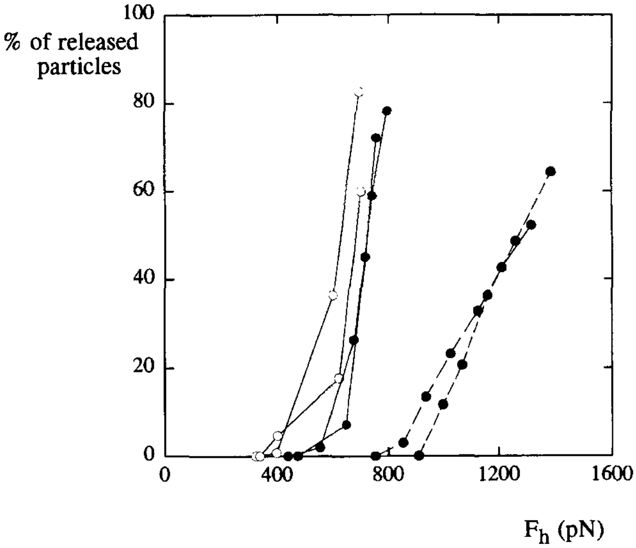

Fig. 7 Experimental detachment curves of bare silica particles from the capillary surface saturated by cat5 (straight lines) and cat100 (dotted lines). The adhesive force derived is 650 pN with cat5 and 1300 pN with cat100, the factor distribution σF is 0.2 with both polyelectrolytes. The value of F_a does not depend on the size of the capillary. The cross-section of capillary used is 200 μm × 4 mm (empty symbols) and 100 μm × 2 mm (filled symbols). For each experiment, $I = 10^{-3}$ M and pH = 6, in maleic buffer

Polymer and detachment force distribution

With bare surfaces, two parameters were proposed to account for a broad distribution of the hydrodynamic strength: the roughness of either surface [51, 52, 54] and a heterogeneous distribution of the surface charges [53]. The presence of adsorbed polymer is expected to influence both of them. First, asperities may be hidden by the polymer layer if it is thick enough compared to λ, narrowing the force distribution. This was actually observed with the three polymers we used. A comparison between POE2M and cat100 shows that despite an equal layer thickness (10 nm), the reduction in σ_F was much more pronounced with the cationic polymer than with the neutral one: $\sigma_F = 0.8$ with POE2M and $\sigma_F = 0.2$ with cat100. On the contrary, cat5 and cat100 led to the same decrease of σ_F ($\sigma_F = 0.2$), although the layer thicknesses were quite different ($\delta_h = 75$ nm and $\delta_h = 10$ nm respectively). This shows the predominant role of the second parameter, the charge distribution, and has to be correlated again to zeta potential measurements. Low values of the distribution factor σ_F always correspond to very thin mobility spectra. When covered with polyelectrolytes, the charge density of particles is increased and appears more homogeneous from the outer surface. Furthermore, particles are described as tethered to the surface by an entangled bundle of polymer chains [55]. As a consequence the contact area between the particle and the plane surface is increased which also softens the effect of the discrete repartition of charges.

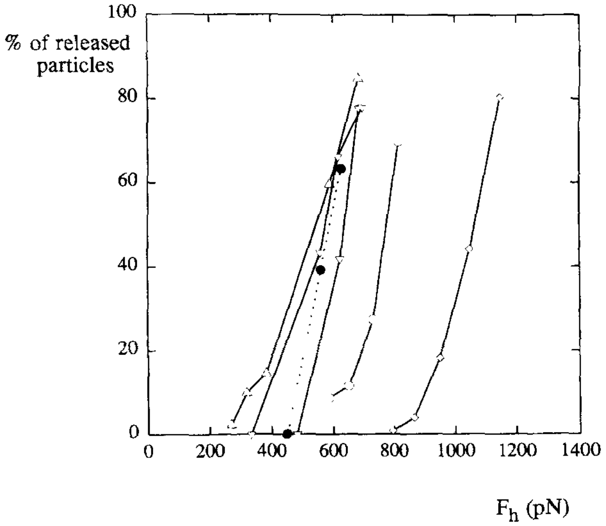

Fig. 8 Experimental detachment curves of silica particles with various amount of adsorbed cat5 polymer from fully covered capillary surface ($I = 10^{-3}$ M and pH = 6, in maleic buffer). Bare particles are shown by filled symbols. The initial polymer dose is 0.4 mg/m^2 (◇), 0.5 mg/m^2 (○), 0.75 mg/m^2 (▽) and 1 mg/m^2 (△), the particle concentration during the polymer adsorption step is 0.14 g/l. The distribution factor σF is 0.2 for each experiment

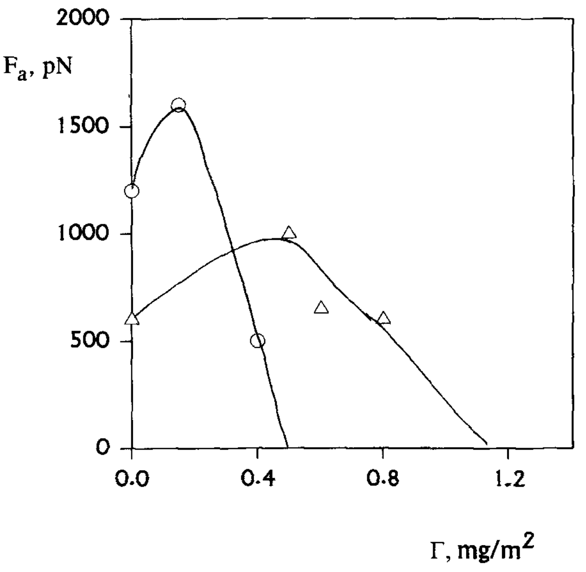

Fig. 9 Variation of the adhesive force measured between fully saturated capillary and silica particles with various coverage at pH6 and $I = 10^{-3}$ M in maleic buffer. This force exhibited a maximum at intermediate particle coverage for both polymer cat5 (△) and cat100 (○). The lines are drawn as a guide for the eye

Particle adhesion and flocculation of suspensions

In order to reproduce particle aggregation, we attempted to estimate the adhesive force when polymer was adsorbed on both surfaces. In the following experiments, the capillary surface was fully covered (because an intermediate coverage could not be controlled) while the particle coverage varied from bare to saturated.

Figure 8 shows the detachment curves obtained in the case of the cat5 copolymer. The stiffness of the experimental curves ($\sigma F = 0.2$) guarantees the homogeneous coverage of both surfaces (particles and plane) which represents the major difficulty of such experiments. The adhesive force exhibits a maximum value as a function of particle coverage, as depicted in Fig. 9 for cat5 and cat100 copolymers. This maximum can be linked to the optimal flocculation efficiency in silica suspensions. Let us consider the global amount of polymer adsorbed on both surfaces: we define an average coverage rate, Γ_{ave}, as the half-sum of both separate coverage rates, Γ_{cap} and Γ_{beads}. This parameter can then be compared to the coverage rate of the beads within a suspension. For both polyelectrolytes cat5 and cat100 the maximum in the adhesive force falls in the flocculation zone observed in suspension, which reveals that both phenomena are quantitatively linked.

As the detachment of silica particles was very sensitive to the amount of polymer adsorbed, we used that methodology to investigate the repartition of adsorbed polymers throughout flocculated suspensions. Semi-dilute suspensions (1.4 g/l) of silica beads were prepared at low cationic copolymer cat5 doses (0.5 and 0.65 mg/m^2) in order to promote aggregation without an excess of polymer. Polymer/particle mixtures were stirred during 1 h

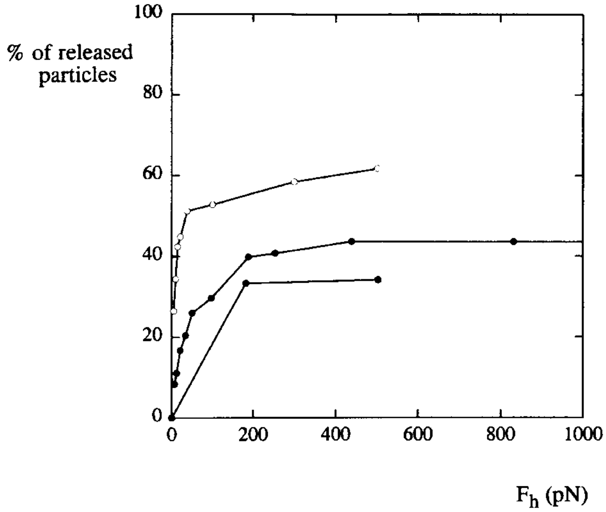

Fig. 10 Experimental detachment curves of silica particles belonging to flocculated suspensions. The polymer dose is 0.5 mg/m^2 (empty circles) and 0.65 mg/m^2 (filled circles) and the particle concentration is 1.4 g/l. The unusual look of the detachment curves is characterized by an infinite distribution factor. These curves reflect the heterogeneity of the copolymer repartition throughout the suspension due to the coupling between the polymer adsorption and the particle aggregation

and sonicated just before measurements. Particles were then injected in a bare capillary. The unusual appearance of the detachment curves depicted in Fig. 10 and characterized by an infinite distribution factor σ_F reflects the heterogeneity of the copolymer repartition throughout the suspension. Indeed, some of the beads were only slightly covered and could be removed from the capillary surface, while 40 to 60% of them could not, indicating a higher coverage. This heterogeneous repartition of polymer among particles of flocculated suspensions had been previously evidenced in semi-dilute or concentrated suspensions [47]. Aggregation was possible in the first stage of the mixing when polymer chains were still in a non equilibrium configuration, being able to build bridges between the particles. Stirred suspensions prepared with a low polymer dose and a high particle concentration are favorable conditions for such an aggregation mechanism. As a consequence particles trapped inside the aggregates are less covered than particles located outside the aggregates.

Conclusion

Based on the detachment of spherical particles from a planar surface with polymer possibly adsorbed on it, the device we built appeared as a good tool to investigate the influence of various adsorbed polymers on the adhesion and removal of particles.

The deposit of bare particles on bare surface was governed by the pH and the ionic strength. Adhesion of particles was well described by the DLVO theory and by ζ-potential measurement. The hydrodynamic detachment of adhering particles was determined by the roughness of the surfaces, which fixed the contact area between the sphere and the plan. If surfaces were not completely smooth, then detachment was sensitive to the number of charges belonging to the contact area and consequently sensitive to the pH and ionic strength conditions. The distribution of the detachment force was then interpreted as a nonuniformity of these charges. Recent experimental results published after we finished this work could confirm this interpretation [53]. These authors studied the influence of pH on the hydrodynamic detachment of glass spheres from a flat glass surface. Their results show that the adhesive force decreased when the pH increased from 3 to 6 due to the electrostatic repulsions between more and more charged surfaces. We derived the distribution factor from the experimental results described in this paper. We found that this factor was around 1 at pH 3 whatever the size of the beads. On the contrary, experiments performed at pH 5 or 6 were characterized by a distribution factor of 3 and 4 respectively. Finally, when low-charged surfaces were involved the detachment force was rather high and characterized by a low distribution factor because even if charges are not homogeneously distributed, the number of charges was not sufficient to influence the detachment force. With moderate-charged surfaces the detachment force was low and the distribution factor was high due to the non-uniformity of charges over the surfaces. With very high-charged surfaces, particles did not attach to the flat surface.

Adsorption of a neutral polymer did not significantly change the surface charge, thus adhesion of Brownian particles occurred when the polymer layer thickness is larger than the Debye–Hückel length. The influence of neutral polymers on the particle detachment was found to depend on the size of the beads. The difference we observed between Brownian particles (silica beads) and non-Brownian particles (glass beads) showed that the compression of the polymer layer under the pressure exerted by the particles themselves could considerably enhance the particle adhesion. With the larger glass particles, detachment was sensitive to the molecular weight of neutral polymer because the number of bridges between surfaces increased with M_w. With Brownian silica beads, the major effect was obtained when using high molecular weight polyelectrolytes. The adhesion force was drastically enhanced even with copolymers of low cationicity rate (5%), showing the efficiency of electrostatic interactions. A parallel was drawn between electrophoretic mobility and particle detachment measurements. In both of them, the distribution of charges throughout the polymer layer and at its outer surface appeared as a major factor which influenced the experimental results.

As detachment measurements were very sensitive to the amount of adsorbed polymers – especially with polyelectrolytes – our methodology could be used to evidence an heterogeneous repartition of polymer inside flocculated suspensions. This repartition results from the coupling between polymer adsorption and particle aggregation [47]. If bridging between particles occurs when polymer chains are in a non equilibrium conformation, then particles trapped inside the aggregates have rather low coverage while particles located outside the aggregates are more covered.

Acknowledgments This work was financially supported by the GDR project "Filtration/Fibres creuses" of the Centre National de la Recherche Scientifique, in collaboration with "Lyonnaise des Eaux". We also thank Rhône-Poulenc for giving us access to their zetameter device (model 3000).

References

1. Bowen WR, Jenner F (1995) Adv in Colloid Interface Sci 56:141
2. Baudin I, Millequant M, Ricard A, Audebert R (1992) Desalination 86:237
3. Luckham PF, Hartley PG (1994) Adv in Colloid Interface Sci 49:341
4. Claesson M, Blomberg E, Fröberg JC, Nylander T, Arnebrant T (1995) Adv in Colloid Interface Sci 57:161
5. Chenu C, Guerif J (1991) Soil Sci Soc of America J 55:1076
6. Luckham PF, Costello BADL (1993) Adv in Colloid Interface Sci 44:183
7. De Mejo LP, Rimai DS, Chen J, Bowen RC (1992) J Adhes 39:61
8. Li YQ, Tao NJ, Pan J, Garcia AA, Lindsay SM (1993) Langmuir 9:637
9. Mizes H (1992) Proceedings of the 23rd Annual Meeting of the fine Particle Society
10. Götze T, Rabinovitch YI, Sonntag H (1987) Colloid and Polym Sci 265:134
11. Israelachvili JN, Adams GE (1973) J Chem Soc Farad Trans I 74:975
12. Derjaguin BV, Landau LD (1941) Acta Phys Chim URSS 14:663 Verwey EJW, Overbeeck JThG (1948) Theory of the Stability of Lyophobic Colloids Elsevier Amsterdam (1948)
13. Horn RG, Smith DT (1990) J of noncrystalline Solids 120:72
14. Toikka G, Hayes RA, Ralston J (1996) J Colloid Interface Sci 180:329
15. Klein J, Luckham PF (1982) Nature 300:429
16. Lubetkin S (1988) Colloids and Surfaces 31:203
17. Luckham PF, Klein J (1985) Macromolecules 18:721
18. Taunton HJ, Toprakcioglu C (1988) Colloids and Surfaces 31:151
19. Costello BADL, Luckham PF, Tadros TF (1993) J Colloid Interface Sci 156:72
20. Götze T, Sonntag H (1988) Colloids and Surfaces 31:181
21. Klein J, Luckham PF (1984) Macromolecules 17:1041
22. Claesson PM (1993) Colloids and Surfaces A 77:109
23. Kurihara K, Kunitake T (1992) Langmuir 8:2087
24. Luckham PF, Klein J (1984) J Chem Soc Farad Trans I 80:865
25. Afshar-RAd T, Bailey AI, Luckham PF, Macnaughtan W, Chapman D (1988) Colloids and surfaces 31:125
26. Dix LR, Toprkcioglu C, Davies RJ (1988) Colloids and Surfaces 31:147
27. Dahlgreen M (1994) Langmuir 10:1580
28. Dahlgreen M, Waltermo A, Blomberg E, Claesson PM (1993) J Chem Phys 97:11769
29. Claesson M, Christenson HK, Berg JM, Neuman RD (1995) J Colloid Interface Sci 172:415
30. Luckham PF (1991) Adv in Colloid and Interface Sci 34:191
31. Dahlgreen M, Claesson PM, Audebert R (1993) Nordic Pulp & Paper Research Journal 1:6267
32. Pelton RH, Allen LH (1984) J Colloid Interface Sci 99:387
33. Mühle K (1985) Colloid and Polymer Sci 263:660
34. Visser J (1970) J Colloid Interface Sci 34:26
35. Pelton RH, Nugent H, Allen LH (1982) Colloids and Surfaces 4:397
36. Sjollema J, Buscher HJ, Weerkamp AH (1989) J Microbiol Methods 73
37. Varennes S, Van de Ven TGM (1988) Colloids and Surfaces 33:63
38. Visser J (1976) J Colloid Interface Sci 55:664
39. Zimon AD (1982) "Adhesion of dust and Powder" consultants bureau, New York
40. St John DF, Montgomery DJ (1971) J Appl Phys 42:663
41. Meinders JM, Busscher HJ (1994) Colloid & Polym Sci 272:478
42. Hübbe MA (1987) Colloids and Surfaces 25:311 and 325
43. Varennes S, Van de Ven TGM (1988) Physico Chemical Hydrodynamics 10: 415
44. Elzo D, Schmitz P, Houi D, Joscelyne S (1996) J of Membrane Sci 109:43
45. Goldman AJ, Cox RG, Brenner H (1967) Chem Eng Sci 22:653
46. Unger KK, Jilge G (1986) J of Chromatography 359:61
47. Chaplain V, Janex ML, Lafuma F, Graillat P, Audebert R (1995) Colloid and Polymer Sci 273:984
48. Mabire F, Audebert R, Quivoron C (1984) Polymer 25:1317
49. Lee JJ, Fuller GG (1984) J Colloid and Interface Sci 103:569
50. Hsu JP, Fan YP (1995) J Colloid and Interface Sci 172:230
51. Sharma MM, Chamoun H, Sita Rama Sarma DSH, Schechter S (1992) J Colloid and Interface Sci 149:121
52. Hubbe MA (1984) Colloids and Surf 12:151
53. Yiantsios SG, Karabelas AJ (1995) J Colloid and Interface Sci 176:74
54. Das SK, Schechter RS, Sharma MM (1994) J Colloid and Interface Sci 164:63
55. Dabros T, Warszynski P, Van de Ven TGM (1994) J Colloid and Interface Sci 162:254